

Article

Information Entropy of Regular Dendrimer Aggregates and Irregular Intermediate Structures

Denis Sabirov , Alina Tukhbatullina  and Igor Shepelevich

Institute of Petrochemistry and Catalysis, Russian Academy of Sciences, 450075 Ufa, Russia; kalieva.alina@rambler.ru (A.T.); shepelevichis@mail.ru (I.S.)

* Correspondence: diozno@mail.ru; Tel.: +7-(347)-2842750

Abstract: Dendrimer molecules and aggregates are chemical structures with regular branching that underlies their physicochemical properties. Regular dendrimers have been studied both theoretically and experimentally, but the irregular intermediate structures between the dendrimers of neighboring generations have not. In the present work, dendrimer aggregates, both regular and intermediate, are investigated in terms of the information entropy approach. As found, the information entropy of the regular dendrimer asymptotically increases with the generation number; herewith, its maximal value equals 2. The intermediate structures have been studied for the growing dendrimer $G1 \rightarrow G2 \rightarrow G3 \rightarrow G4$ with the tricoordinated building block. The plot of the information entropy of the growing dendrimer on the size has the frontier consisting of the lowest values that correspond to the regular and irregular structures described with the symmetrical graphs. Other intermediate structures have information entropies higher than the regular dendrimers. Thus, to move the system from one informationally stable state to another, its information capacity must be temporarily increased.

Keywords: dendrimer; regular dendrimer; intermediate structure; aggregation; information entropy



Citation: Sabirov, D.; Tukhbatullina, A.; Shepelevich, I. Information Entropy of Regular Dendrimer Aggregates and Irregular Intermediate Structures. *Liquids* **2021**, *1*, 25–35. <https://doi.org/10.3390/liquids1010002>

Received: 13 January 2021

Accepted: 3 March 2021

Published: 5 March 2021

Publisher's Note: MDPI stays neutral with regard to jurisdictional claims in published maps and institutional affiliations.



Copyright: © 2021 by the authors. Licensee MDPI, Basel, Switzerland. This article is an open access article distributed under the terms and conditions of the Creative Commons Attribution (CC BY) license (<https://creativecommons.org/licenses/by/4.0/>).

1. Introduction

Fractals are mathematical objects made up of patterns manifesting self-similarity [1]. Ideal fractals exist only in the mind, but the concept provides useful approaches for describing real chemical objects with a highly branched structure. Chemical fractals are regular molecules or supramolecular species with repeated patterns, usually synthesized in solutions or precipitated from them [2]. The repeated nature comes from the chemical features of their building blocks (chemical groups or molecules), which associate in line with strict rules, *viz.*, each block is coordinated (or chemically bonded) with the constant number of other blocks, and this coordination number is reproduced at each step of aggregation. Branched colloid and surface aggregates (e.g., colloid nanoaggregates of gold [3,4] and fullerenes [5,6], electrochemically generated ammonia amalgam [7], dendrites grown on inorganic templates [8,9]) or dendrimer molecules (multi-cage fullerene-containing branched molecules [10–12] or single-cage fullerene derivatives structuring surrounding molecules [13], branched organic [14,15], and organoelement [16,17] polymers etc.) are typical examples of chemical fractals. Currently, the concepts of fractals and dendrimers are used in synthetic chemistry for the structural design of novel substances and materials with tunable properties (see the relevant reviews [18–22]).

Chemical fractals and dendrimers have become the objects of theoretical research, including their treatment in terms of the graph and information theories [23–29]. Typically, rationalizing their topology is based on the calculations of structural descriptors. Branching is usually considered as a kind of order that could be described with entropy values associated with the graph relevant to the chemical structure [23,24]. Notably, information entropy in its simple form (or Shannon entropy) is the kernel for other entropy descriptors [30–34]. On the other hand, it may relate to real processes occurring in chemical systems, including

the processes of self-assembly [35–38]. Therefore, in our work [39–44], we focus on the information entropies of chemical particles.

Mathematical properties of the information entropies of dendrimers have been deeply studied by Chen et al. [23] and Ghorbani et al. [24], focusing on symmetric graphs corresponding to dendrimers with a regular topology.

We briefly note that other theoretical approaches that are invoked to scrutinize the dendrimer growth and molecular dynamics techniques are some of the most efficient tools for this purpose [45,46].

In the present work, we use a simple dendrimer model to rationalize its information entropy in the context of physicochemical properties and, for the first time, consider imperfect dendrimers, intermediates between two generations of regular dendrimers.

2. Description of the Mathematical Model

2.1. Basic Definitions

We consider the dendrimer aggregate formed with identical building blocks, which are chemically indistinguishable and have the same coordination number, b . This means that, in the corresponding graph, each block is connected to other b blocks. We exemplify this model with the graph corresponding to the dendrimer with $b = 3$ (Figure 1). This is the minimal b value when the dendrimer model is meaningful. The dendrimer is divided into n shells, where n is called the generation number in synthetic chemistry [14–22] (in some theoretical works, it is also called a radius of the graph [23]). Note that the free blocks are identical but they become different when included in the dendrimer, depending on the number of shells they belong to. Within i -th shells, all blocks are identical and their number equals ba^{i-1} (except for the 0-th shell, which consists of a single block). Hence, the total number of blocks in the dendrimer of generation n is:

$$N = 1 + \sum_{i=1}^n ba^{i-1} = 1 + \frac{b(a^n - 1)}{a - 1}. \quad (1)$$

Each block of the i -th shell is connected to one block of the $(i - 1)$ -th shell, and $a = b - 1$ blocks belonging to the $(i + 1)$ -th shell. The prevalence of connecting with outer shells underlies the branched structure, and we call a the parameter of branching. Notably, in real chemical systems, both fractal aggregates and dendrimer molecule, b and n , values are not large numbers due to the steric hindrances [14–22].

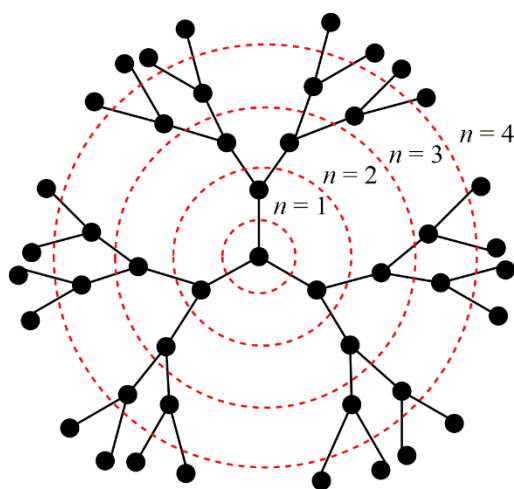


Figure 1. The dendrimer of generation $n = 4$ with coordination number of building blocks $b = 3$.

2.2. Information Entropy of Dendrimer

According to the original Shannon approach, we select the particle n types of identical building blocks (atoms, monomer units, etc.), and the information entropy of the particle is defined as:

$$h = - \sum_{i=1}^n \frac{N_i}{N} \log_2 \frac{N_i}{N}, \quad (2)$$

where N_i denotes the number of building blocks of the i -th type and N is their total number ($N = \sum N_i$). In the dendrimer structure introduced in Section 2.1 (Figure 1), we select one vertex of the 0-th shell (the starting point of the dendrimer growth), N_1 vertices of the 1st shell, N_2 vertices of the 2nd shell, and ... N_n atoms of the n -th shell. The conventional designation of such partition is: $1 \times 1 + 1 \times N_1 + 1 \times N_2 + \dots + 1 \times N_n$ (that corresponds to [number of types] \times [number of blocks within the type]; see [39,40]). Applying Equation (1) to this partition provides the information entropy, h , of the dendrimer as a sum of the logarithms of the weights:

$$h = - \frac{1}{N} \log_2 \frac{1}{N} - \sum_{i=1}^n \frac{ba^{i-1}}{N} \log_2 \frac{ba^{i-1}}{N}. \quad (3)$$

The weights of the blocks from each shell (N_i/N , $i = 0, \dots, n$) may be interpreted as the probabilities to find the block of the i -th type in the structure, and

$$\sum_{i=0}^n \frac{N_i}{N} = 1. \quad (4)$$

To apply this approach to routinized calculations, expression (3) should be simplified to be more convenient. We present it in the following form (the transformation of Equation (3) is shown in Supplementary Materials, Section A):

$$h = h_{max} + h_{fract}, \quad (5)$$

where

$$h_{max} = \log_2 N \quad (6)$$

and

$$h_{fract} = \frac{N-1}{N} \log_2 \frac{a}{b} - \frac{b}{N} \frac{na^{n+1} - (n+1)a^n + 1}{(a-1)^2} \log_2 a \quad (7)$$

Two terms of the derived Equation (5) have a physicochemical (structural) interpretation. The term h_{max} is positive and corresponds to the highest information entropy value that could be achieved if N blocks are united randomly, so that all units of the formed aggregate differ. The second term, $h_{fract} < 0$, is the information entropy of fractalization that shows the decrease in the information entropy of the system due to the formation of a fractal pattern. Note that the model is relevant to both dendrimer molecules and fractal aggregates; i.e., it works regardless of the type of the bonds (chemical bonds or intermolecular interactions, respectively) connecting the units of the particle.

In the case of $b = 2$, we obtain a linear structure instead of a dendrimer. This linear polymer contains $N = 2n + 1$ building blocks, as follows from Equation (1). According to Equations (6) and (7), the h_{max} and h_{fract} values equal:

$$h_{max} = \log_2(2n + 1) \quad (8)$$

and

$$h_{fract} = - \frac{2n}{2n + 1} \quad (9)$$

Two latter equations are the same as the expressions obtained for the linear polymer with the odd number of building blocks in terms of the general definition of information entropy and Equation (2) (Supplementary Materials, Section B).

3. Results and Discussion

3.1. Upper Bound of the Information Entropy of Dendrimer at the Infinite Generation Number

We used Equations (5)–(7) to scrutinize the behavior of the information entropy of the dendrimer upon the infinitely increasing generation number. As mentioned above, the generation numbers of the synthesized dendrimer molecules are not large, so assessing the upper bounds, h_∞ , primarily relates to the theoretical interest. On the other hand, the potential applications of dendrimers include information storage with nanopatterned materials [21]. As information entropy of a material is relevant to its information capacity [45], the limit values, h_∞ , may also be used as waymarks in this direction.

We found that dependences, $h = f(n)$ with b as a parameter, are increasing asymptotic curves (Figure 2). We were able to determine the corresponding limit values, h_∞ , only numerically: 2 ($b = 3$), 1.377 ($b = 4$), 1.082 ($b = 5$), and 0.902 bits ($b = 6$). Thus, h_∞ decreases with increasing b (Figure 3), and this behavior is explainable. Indeed, each next shell of the dendrimer contains a higher number of similar building blocks. It makes the dendrimer structure more homogeneous at each next generation, and the homogeneity is reached faster with higher b values, which is reflected with h values. Interestingly, the highest possible information entropy in the class of dendrimers corresponds to the simplest case of $b = 3$; i.e., it corresponds to the structures with minimal branching.

The asymptotic behavior of functions $h = f(n)$ indicates that the information entropy becomes independent of the generation number upon the dendrimer growth (Figure 2). The existence of the asymptotic values (h_∞) qualitatively relates to the experimental results. For example, the regularities of the processes of dendrimer formation have similar asymptotic behaviors such as velocity of the growth of silver dendrites upon precipitation [9] and dependence of the fractal dimension of the epitaxially grown fullerene nanoaggregates on the number of layers [8]. Additionally, the electro-optical properties of organic dendrimers with rigid structures are almost independent of the generation number (e.g., dendrimers from bithiophenesilane [14] and fulleropyrrolidine-containing poly(benzyl ether) [11]). At the same time, if the chemical structure of a dendrimer is conformationally flexible, the generation number defines the properties [14].

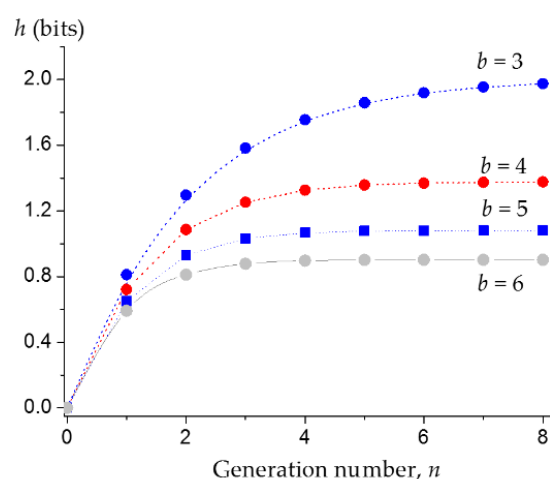


Figure 2. The dependences of information entropy of the dendrimers with various coordination numbers of building blocks, b , on the generation number. Numerical data associated with the plots can be found in Supplementary Materials (Section C).

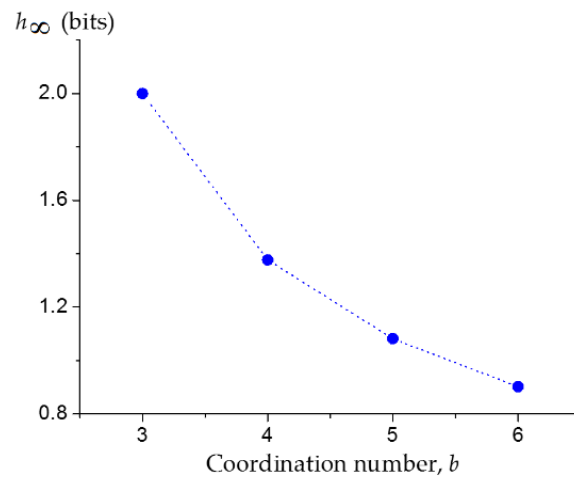


Figure 3. The dependence of the limit information entropy, h_∞ , of dendrimers on the coordination number.

3.2. Imperfect Dendrimers and Information Entropy of Intermediate States

Previous works on the topology of dendrimers have been devoted to the structures with fulfilled shells. However, the next generation of a dendrimer is not produced in one step, so that intermediate imperfect structures are formed when filling the shells. We consider, in general, the issue of intermediate structures between generations G_n and $G_{(n+1)}$. For this purpose, we introduce the rules of filling the shells relating to the chemical features of the aggregation process and consider its two modes.

According to path I, the filling starts from any building block (due to their equivalence) of the outer shell number n . The blocks of outer shells are able to attach a novel blocks, which will form the shell number $(n+1)$. First, the coordination number of this block is completely saturated and then the same processes start via the neighboring block (neighboring means that both blocks of shell n are coordinated with the same block of the shell $(n-1)$). This aggregation mode implies that the new shell is completed in the first dendron and only then starts growing in the next one. According to this mode, building blocks with a lower number of uncompensated valences have higher reactivity toward free blocks. As an example, we consider such a process for dendrimer growth $G_1 \rightarrow G_2 \rightarrow G_3 \rightarrow G_4$ with $b = 3$ (Figure 4).

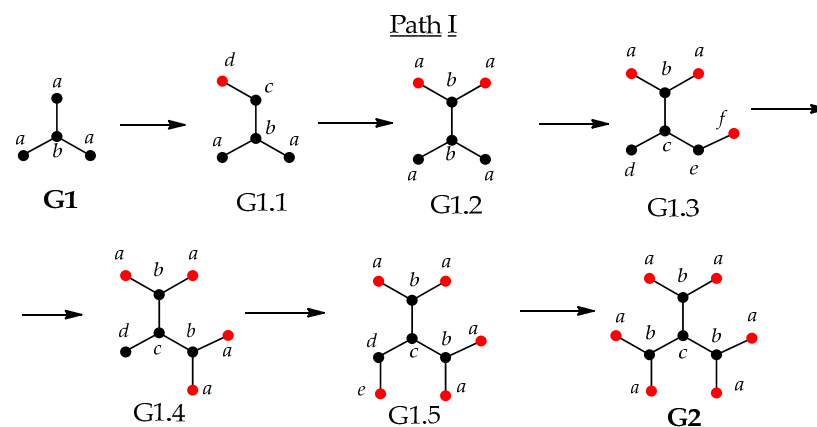


Figure 4. Cont.

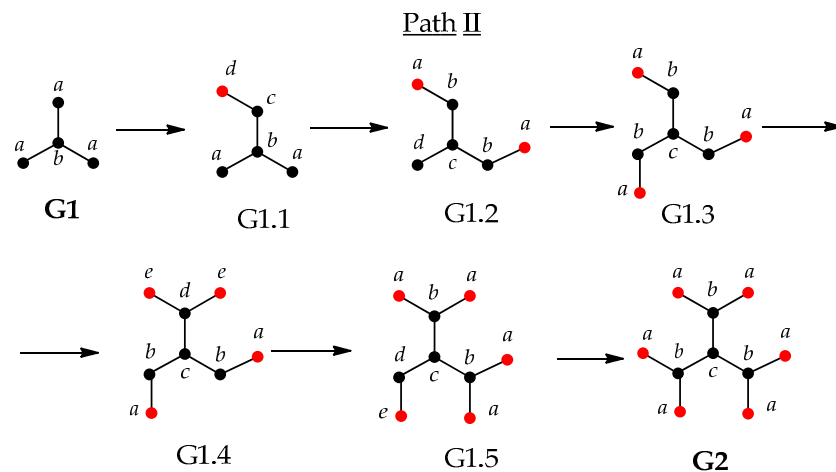


Figure 4. Schematic of two paths of transformation $G1 \rightarrow G2$ (new added blocks are shown in red hereinafter, and the blocks are lettered according to the equivalence of their positions).

Path II corresponds to another reactivity ratio; building blocks with a lower number of uncompensated valences have lower reactivity toward free blocks. Therefore, free blocks are attached to “bare” blocks of the outer shell (Figure 4). In line with both modes, we fill the growing shells traversing clockwise the terminal vertices of the dendrimer graph.

Figure 4 demonstrates that discriminating the blocks according their equivalence does not coincide with their belonging to the shells. Hence, to calculate the information entropies of the intermediate structures, we use the expression for information entropy in a general view (Equation (2)). The obtained numerical results for the dendrimer growth, $G1 \rightarrow G2 \rightarrow G3 \rightarrow G4$, with $b = 3$ are collected in Supplementary Materials (Sections D–I), and here we present their graphical representations as the function $h = f(N)$ (Figure 5). In general, the plots associated with the two paths differ. Only the points corresponding to regular structures $G1, G2, G3$, and $G4$ (dendrimers with completely fulfilled outer shells) take the same positions on the plots.

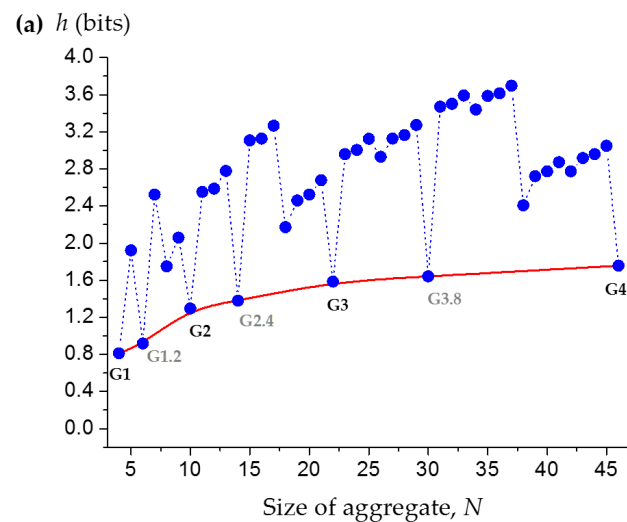


Figure 5. *Cont.*

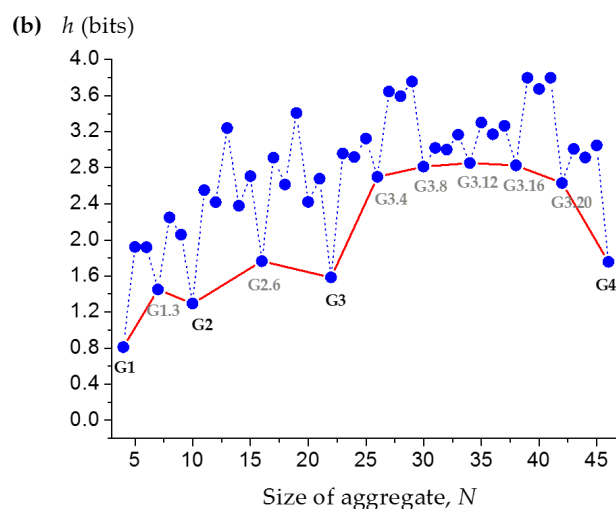


Figure 5. Information entropy upon dendrimer growth, $G1 \rightarrow G2 \rightarrow G3 \rightarrow G4$, according to modes I (a) and II (b). Blue dotted lines show the stepwise h change; red solid lines correspond to the frontier of lower values h_{front} upon the growth. The points of the frontier are labeled with the codes of the structures shown in Figures 6 and 7. Numerical data associated with the plots can be found in Supplementary Materials (Sections D–I).

The frontiers of lower h values (h_{front}) can be selected in the plots of h as a function of the number of building blocks, N , in the growing structures (Figure 5). The frontiers involve the values corresponding to regular dendrimers and intermediates with incomplete outer shells, which manifest the symmetry of their graphs (Figures 6 and 7). We should note that we distinguish these points, not in a strict mathematical manner, but in a chemical sense: the h values of these symmetric structures are substantially lower compared with other intermediates. The frontiers of the two modes of the dendrimer growth differ. In the case of mode I, the information entropy monotonously increases all the way, $G1 \rightarrow G2 \rightarrow G3 \rightarrow G4$. In the case of the alternative mode II, the frontier has the minima corresponding to the regular dendrimers and is separated by other points meeting the criteria $h_i > h_{Gn}$, $h_i > h_{G(n+1)}$ for $N_{Gn} < N_i < N_{G(n+1)}$. Function $h_{front} = f(N)$ is not monotonous due to the latter values attributed to the intermediate structures.

Thus, the different reactivity of the terminal building blocks of the dendrimer is reflected with the type of the functions, $h = f(N)$ and $h_{front} = f(N)$. In general, the transit between the neighboring generations of the dendrimer proceeds through the intermediate structures, which mostly have higher information entropies than the regular structures. This means that we must temporarily increase the information capacity of the system to move the system from one informationally stable state to another (or in terms of the information theory [47], the description of at least one intermediate between two stable states requires larger information resources compared with the stable states themselves).

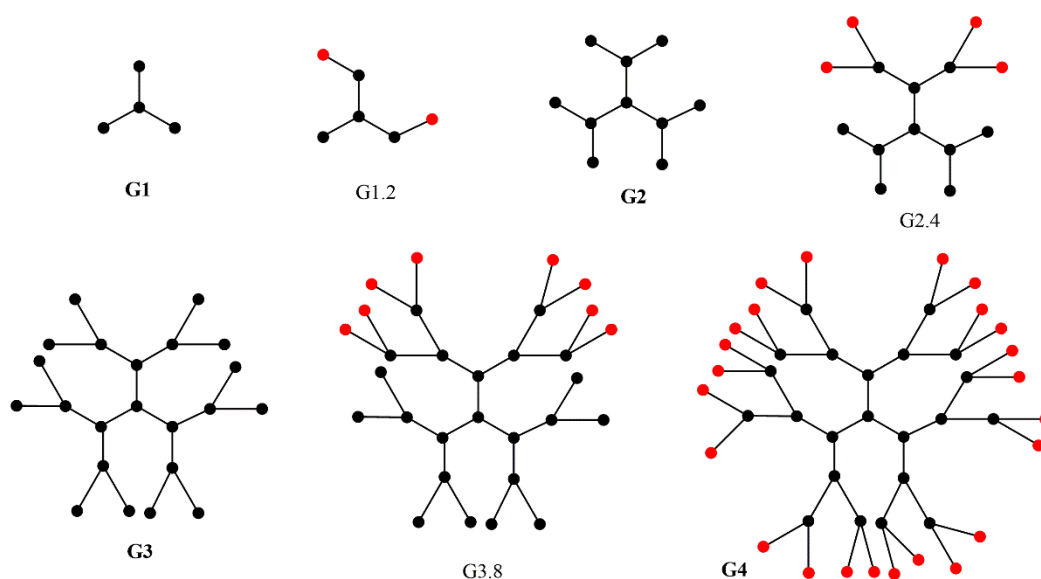


Figure 6. The regular and intermediate structures, in which h values form lower frontier $h_{front} = f(N)$ upon $G1 \rightarrow G4$ transformation via path I.

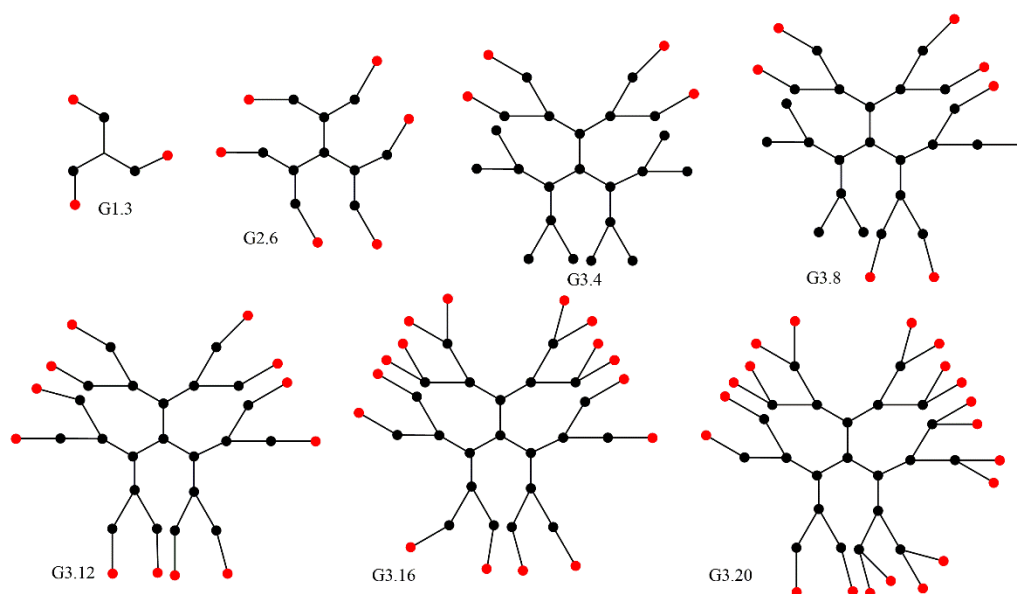


Figure 7. The intermediate structures, in which h values form lower frontier $h_{front} = f(N)$ upon $G1 \rightarrow G4$ transformation via path II.

4. Prospective

We propose that our theoretical findings will stimulate further studies of dendrimers in the aspects of their numerical modeling and material science. Symmetrical and homogeneous chemical systems manifest low information entropies, and vice versa [39–44]. The information entropy of fractal structures, according to Equations (5)–(7), represents the balance between order ($h_{fract} < 0$) and disorder ($h_{max} > 0$) and may be used in structural design for numerical assessment of this balance. This could be useful in the context of using dendrimers as energy-storage materials [48] or within the conception of meso-entropic materials [49]. This additionally requires scrutinizing the correlations between the h values and other branching parameters [50].

Thermodynamic entropy becomes a part of molecular dynamics studies on complex chemical systems; e.g., thermodynamic entropy of enzyme–substrate complexations [51,52]

or configuration entropy of glass-forming liquids [53]. Analogous simulations, with the information entropy as a critical structural criterion, could be a new step in this direction.

5. Conclusions

We have used analytical expressions $h = f(n)$ to demonstrate numerically that the information entropy of a dendrimer approximates to the limit value at the infinite generation number. The limit value is maximal and equal to 2 in the case of tricoordinated building blocks ($b = 3$).

For the first time, we have studied the irregular intermediates between the dendrimers of stepwise generations. We have found that size-dependencies, $h = f(N)$, are defined with the rules of filling the dendrimer shells (deduced from the reactivity of its terminal building blocks). In $h = f(N)$, we select the frontier of the lowest h values corresponding to the regular dendrimer and irregular structures, which are described with the symmetrical graphs. Other intermediate structures have information entropies higher than the values of the regular dendrimers; hence, additional information capacity is required to switch the system between the informationally stable states.

We propose that the theoretical findings of this work will stimulate further studies of dendrimers regarding their material science applications [21,46].

Supplementary Materials: The following are available online at <https://www.mdpi.com//1/1/2/s1>, Sections A–I.

Author Contributions: Conceptualization, D.S.; methodology, D.S.; validation, A.T. and I.S.; formal analysis, A.T.; investigation, D.S. and A.T.; resources, I.S.; writing—original draft preparation, D.S. and A.T.; writing—review and editing, I.S.; visualization, A.T.; supervision, D.S.; project administration, D.S.; funding acquisition, D.S. All authors have read and agreed to the published version of the manuscript.

Funding: This research was partly funded by the Council of the Grants of the President of RF, grant number MD-874.2021.1.3.

Institutional Review Board Statement: Not applicable.

Informed Consent Statement: Not applicable.

Acknowledgments: The work has been performed under the theme ‘Novel theoretical approaches and software for modeling complex chemical processes and compounds with tunable physicochemical properties’ (registration number AAAA-A19-119022290011-6, Russian Federation).

Conflicts of Interest: The authors declare no conflict of interest.

References and Note

1. Mandelbrot, B. *The Fractal Geometry of Nature*; W. H. Freeman and Company: New York, NY, USA, 1982; pp. 1–468.
2. Lazzari, S.; Nicoud, L.; Jaquet, B.; Lattuada, M.; Morbidelli, M. Fractal-like structures in colloid science. *Adv. Colloid Interface Sci.* **2016**, *235*, 1–13. [[CrossRef](#)]
3. Cheng, W.; Dong, S.; Wang, E. Spontaneous fractal aggregation of gold nanoparticles and controlled generation of aggregate-based fractal networks at air/water interface. *J. Phys. Chem. B* **2005**, *109*, 19213–19218. [[CrossRef](#)] [[PubMed](#)]
4. Singh, A.; Khatun, S.; Gupta, A.N. Anisotropy versus fluctuations in the fractal self-assembly of gold nanoparticles. *Soft Matter* **2020**, *16*, 7778–7788. [[CrossRef](#)]
5. Eletsii, A.V.; Okun, M.V.; Smirnov, B.M. Growth of fractal structures in fullerene solutions. *Phys. Scr.* **1997**, *55*, 363–366. [[CrossRef](#)]
6. Peidys, D.A.; Mosunov, A.A.; Mykhina, Y.V.; Prylutskiy, Y.I.; Evstigneev, M.P. Fractal C₆₀ fullerene aggregation: Equilibrium thermodynamics approach. *Chem. Phys. Lett.* **2020**, *742*, 137161. [[CrossRef](#)]
7. Klochkovskii, S.P. (private demonstration of the ammonia amalgam growth via the cathodic polarization of a mercury drop in solutions of ammonium salts. When voltage applied, the drop is covered with rapidly growing amalgam branches. The formation of amalgam is accompanied with a pronounced volume increase, which can be 100 times larger than the volume of the initial drop. When voltage switched off, the mercury amalgam is decomposed releasing ammonia and dihydrogen).
8. Nemcsics, Á.; Nagy, S.; Mojzes, I.; Schwedhelm, R.; Woedtke, S.; Adelung, R.; Kipp, L. Investigation of the surface morphology on epitaxially grown fullerene structures. *Vacuum* **2009**, *84*, 152–154. [[CrossRef](#)]

9. Miyashita, S.; Saito, Y.; Uwaha, M. Fractal aggregation growth and the surrounding diffusion field. *J. Cryst. Growth* **2005**, *283*, 533–539. [[CrossRef](#)]
10. Lenoble, J.; Campidelli, S.; Maringa, N.; Donnio, B.; Guillon, D.; Yevlampieva, N.; Deschenaux, R. Liquid–crystalline Janus-type fullerodendrimers displaying tunable smectic–columnar mesomorphism. *J. Amer. Chem. Soc.* **2007**, *129*, 9941–9952. [[CrossRef](#)]
11. Scanu, D.; Yevlampieva, N.P.; Deschenaux, R. Polar and electrooptical properties of [60]fullerene-containing poly(benzyl ether) dendrimers in solution. *Macromolecules* **2007**, *40*, 1133–1139. [[CrossRef](#)]
12. Yin, H.; Wang, M.; Tan, L.-S.; Chiang, L.Y. Synthesis and intramolecular energy- and electron-transfer of 3D-conformeric tris(fluorenyl-[60]fullerenylfluorene) derivatives. *Molecules* **2019**, *24*, 3337. [[CrossRef](#)]
13. Takaguchi, Y.; Hosokawa, M.; Mayahara, M.; Tajima, T.; Sasamori, T.; Tokitoh, N. Formation of zwitterionic fullerodendron using a new DBN-focal dendron. *Sensors* **2010**, *10*, 613–624. [[CrossRef](#)]
14. Yevlampieva, N.P.; Khurchak, A.P.; Borshchev, O.V.; Luponosov, Y.N.; Kleimyuk, E.A.; Ponomarenko, S.A.; Ryumtsev, E.I. Mechanisms of molecular polarization of bithiophenesilane dendrimers in solutions. *Polymer Sci. Ser. A* **2011**, *53*, 569–577. [[CrossRef](#)]
15. Pavlov, G.M.; Korneeva, E.V.; Meijer, E.W. Translational friction of molecules of dendrimers based on poly(propylenimine). *Russ. J. Appl. Chem.* **2000**, *73*, 1784–1788.
16. Zhilitskaya, L.V.; Yarosh, N.O.; Voronkov, M.G. New polyunsaturated organosilicon dendrimers. *Russ. J. Gen. Chem.* **2010**, *80*, 1929–1932. [[CrossRef](#)]
17. Zhilitskaya, L.V.; Istomina, E.E.; Yarosh, N.O.; Voronkov, M.G.; Albanov, A.I.; Yarosh, O.G. Spherical polyunsaturated organosilicon and organogermanium first generation dendrimers of regular structure. *Russ. J. Gen. Chem.* **2006**, *72*, 1864–1869. [[CrossRef](#)]
18. Caminade, A.-M. Inorganic dendrimers: Recent advances for catalysis, nanomaterials, and nanomedicine. *Chem. Soc. Rev.* **2016**, *45*, 5174–5186. [[CrossRef](#)] [[PubMed](#)]
19. Majoral, J.-P.; Caminade, A.-M. Dendrimers containing heteroatoms (Si, P, B, Ge, or Bi). *Chem. Rev.* **1999**, *99*, 845–880. [[CrossRef](#)]
20. Astruc, D.; Boisselier, E.; Ornelas, C. Dendrimers designed for functions: From physical, photophysical, and supramolecular properties to applications in sensing, catalysis, molecular electronics, photonics, and nanomedicine. *Chem. Rev.* **2010**, *110*, 1857–1959. [[CrossRef](#)]
21. Rosen, B.M.; Wilson, C.J.; Wilson, D.A.; Peterca, M.; Imam, M.R.; Percec, V. Dendron-mediated self-assembly, disassembly, and self-organization of complex systems. *Chem. Rev.* **2009**, *109*, 6275–6540. [[CrossRef](#)]
22. Pirozhnikov, P.B.; Korolev, I.V.; Kuzina, N.G.; Mashlyakovskii, L.N. Hyperbranched polymers and their use in the technology of paint-and-varnish materials and coatings. *Russ. J. Appl. Chem.* **2013**, *86*, 1549–1562. [[CrossRef](#)]
23. Chen, Z.; Dehmer, M.; Emmert-Streib, F.; Shi, Y. Entropy bounds for dendrimers. *Appl. Math. Comput.* **2014**, *242*, 462–472. [[CrossRef](#)]
24. Ghorbani, M.; Dehmer, M.; Zangi, S.; Mowshowitz, A.; Emmert-Streib, F. A note on distance-based entropy of dendrimers. *Axioms* **2019**, *8*, 98. [[CrossRef](#)]
25. Jiménez-Ángeles, F.; Odriozola, G.; Lozada-Cassou, M. Entropy effects in self-assembling mechanisms: Also a view from the information theory. *J. Mol. Liquids* **2011**, *164*, 87–100. [[CrossRef](#)]
26. Mitrokhin, Y. Two faces of entropy and information in biological systems. *J. Theor. Biol.* **2014**, *359*, 192–198. [[CrossRef](#)]
27. Liu, J.-B.; Zhao, J.; Min, J.; Cao, J. On the Hosoya index of graphs formed by a fractal graph. *Fractals* **2019**, *27*, 1950135. [[CrossRef](#)]
28. Andriantiana, E.O.D. Energy, Hosoya index and Merrifield–Simmons index of trees with prescribed degree sequence. *Discret. Appl. Math.* **2013**, *161*, 724–741. [[CrossRef](#)]
29. Vesel, A. Linear algorithms for the Hosoya index and Hosoya matrix of a tree. *Mathematics* **2021**, *9*, 142. [[CrossRef](#)]
30. Barigye, S.J.; Marrero-Ponce, Y.; Pérez-Giménez, F.; Bonchev, D. Trends in information theory-based chemical structure codification. *Mol. Divers.* **2014**, *18*, 673–686. [[CrossRef](#)]
31. Basak, S.C.; Niemi, G.J.; Veith, G.D. Predicting properties of molecules using graph invariants. *J. Math. Chem.* **1991**, *7*, 243–272. [[CrossRef](#)]
32. Ghorbani, M.; Dehmer, M.; Emmert-Streib, F. Properties of entropy-based topological measures of fullerenes. *Mathematics* **2020**, *8*, 740. [[CrossRef](#)]
33. Ghorbani, M.; Dehmer, M.; Rajabi-Parsa, M.; Mowshowitz, A.; Emmert-Streib, F. On properties of distance-based entropies on fullerene graphs. *Entropy* **2019**, *21*, 482. [[CrossRef](#)]
34. Ghorbani, M.; Rajabi-Parsa, M.; Mirzaie, R.A. Novel results on entropy-based measures of fullerenes. *Fuller. Nanotub. Carbon Nanostruct.* **2021**. [[CrossRef](#)]
35. Kobozev, N.I. Physicochemical modelling of information and thinking processes. I. Thermodynamics of the information processes. *Russ. J. Phys. Chem. A* **1966**, *40*, 281–284. (In Russian)
36. Zhdanov, Y.A. *Information Entropy in Organic Chemistry*; Rostov University: Rostov-on-Don, Russia, 1979; pp. 1–55.
37. Aleskovskii, V.B. Information as a factor of self-organization and organization of matter. *Russ. J. Gen. Chem.* **2002**, *72*, 569–574. [[CrossRef](#)]
38. Talanov, V.M.; Ivanov, V.V. Structure as the source of information on the chemical organization of substance. *Russ. J. Gen. Chem.* **2013**, *83*, 2225–2236. [[CrossRef](#)]
39. Sabirov, D.S.; Shepelevich, I.S. Information entropy of oxygen allotropes. A still open discussion about the closed form of ozone. *Comput. Theor. Chem.* **2015**, *1073*, 61–66. [[CrossRef](#)]

40. Sabirov, D.S.; Terentyev, A.O.; Sokolov, V.I. Activation energies and information entropies of helium penetration through fullerene walls. Insights into the formation of endofullerenes $nX@C_{60/70}$ ($n = 1$ and 2) from the information entropy approach. *RSC Adv.* **2016**, *6*, 72230–72237. [[CrossRef](#)]
41. Sabirov, D.S. Information entropy change in [2+2]-oligomerization of the C_{60} fullerene. *Int. J. Chem. Model.* **2017**, *9*, 203–213.
42. Sabirov, D.S. Information entropy changes in chemical reactions. *Comput. Theor. Chem.* **2018**, *1123*, 169–179. [[CrossRef](#)]
43. Sabirov, D.S. Information entropy of mixing molecules and its application to molecular ensembles and chemical reactions. *Comput. Theor. Chem.* **2020**, *1187*, 112933. [[CrossRef](#)]
44. Sabirov, D.S.; Koledina, K.F. Classification of isentropic molecules in terms of Shannon entropy. In *EPJ Web of Conferences; EDP Sciences: Les Ulis, France, 2020; Volume 244*, p. 01016. [[CrossRef](#)]
45. Chawla, M.; Kaushik, R.D.; Singh, J.; Manila. Optimization and computational studies evaluating molecular dynamics of EDA cored polymeric dendrimer. *Sci. Rep.* **2020**, *10*, 21977. [[CrossRef](#)]
46. Lee, H.; Larson, R.G. Molecular dynamics simulations of PAMAM dendrimer-induced pore formation in DPPC bilayers with a coarse-grained model. *J. Phys. Chem. B* **2006**, *110*, 18204–18211. [[CrossRef](#)]
47. Nielsen, M.A.; Chuang, I.L. *Quantum Computation and Quantum Information*; Cambridge University Press: London, UK, 2001; pp. 1–822.
48. Bar-Haim, A.; Klafter, J.; Kopelman, R. Dendrimers as controlled artificial energy antennae. *J. Amer. Chem. Soc.* **1997**, *119*, 6197–6198. [[CrossRef](#)]
49. Feng, B.; Zhuang, X. Carbon-enriched meso-entropy materials: From theory to cases. *Acta Chim. Sin.* **2020**, *78*, 833–847. [[CrossRef](#)]
50. Bonchev, D.; Trinajstić, N. On topological characterization of molecular branching. *Int. J. Quant. Chem.* **1978**, *14*, 293–303. [[CrossRef](#)]
51. Graf, M.M.H.; Bren, U.; Haltrich, D.; Oostenbrink, C. Molecular dynamics simulations give insight into D-glucose dioxidation at C2 and C3 by *Agaricus meleagris* pyranose dehydrogenase. *J. Comput. Aided Mol. Des.* **2013**, *27*, 295–304. [[CrossRef](#)] [[PubMed](#)]
52. Putz, M.V.; Lacrama, A.-M.; Ostafe, V. Full analytic progress curves of enzymic reactions in vitro. *Int. J. Mol. Sci.* **2006**, *7*, 469–484. [[CrossRef](#)]
53. Champion, Y.; Thurieau, N. The sample size effect in metallic glass deformation. *Sci. Rep.* **2020**, *10*, 10801. [[CrossRef](#)]